Supporting Information

Grunwald et al. 10.1073/pnas.0912617107

SI Text

SI Materials and Methods. ***Materials.*** All chemicals were obtained from Fluka (Munich, Germany) or Merck (Nottingham, UK) in pro analysis purity. The Fmoc-amino acids Fmoc-Ser(tBu)-OH and Fmoc-His(Trt)-OH were obtained from Rapp Polymere (Tuebingen, Germany), the trityl chloride resins (TCP-resin) from Novabiochem/Merck, and the Fmoc-[S]-3-amino-3-(2nitrophenyl)-propionic acid (Fmoc-Anp) building block from Peptech (Burlington, MA). The ATTO565 dyes were purchased from ATTO-Tec (Siegen, Germany), the Alexa488 dye from Invitrogen (Karlsruhe, Germany), and the Cy5 dye from GE Healthcare (Munich, Germany). The 1-hydroxybenzotriazole (HOBt) was obtained from Alfa Aesar (Karsruhe, Germany), the diamino-polyethylenglycol (diamino-PEG, 2000 kDa) from Rapp Polymere, and the (3-glycidyloxypropyl)-trimethoxysilane from Aldrich (Munich, Germany).

Carboxy-tris-NTA(OtBu). *t*Bu protected, carboxy functionalized tris-NTA [carboxy-tris-NTA(O*t*Bu)] was synthesized as described (1). A further purification step via reversed-phase HPLC on a C_{18} column (Vydac 218TP, Grace) was carried out with a linear gradient from 60–100% acetonitrile in water. Lyophilization leads to the carboxy-tris-NTA(O*t*Bu) as a white powder.

PA tris-NTA synthesis. The four peptidyl-resins were prepared by fully automated solid-phase peptide synthesis using Fmoc/*t*Bu-strategy and Fmoc-His(Trt)-TCP resin. The resin was distributed in 30 mg aliquots (15 μmol) to filter tubes. Fmoc deprotection was carried out two times, 10 min each, with 30% piperidine in DMF (300 μl). Nine washing steps were done with DMF (300 μl). Fmoc-amino acids (0.5 M) were dissolved with HOBt (0.5 M) in DMF. Diisopropylcarbodiimide (DIC) (3 M in NMP, 60 μl) was added to the reaction vessels. Coupling reagents DIC (3 M in DMF, 50 μl, first coupling) or 2-(6-Chloro-1H-benzotriazole-1-yl)-1,1,3,3-tetramethyluronium tetrafluoroborate (TCTU) (0.5 M in DMF, 200 μl, second coupling) and Fmoc-amino acids and Fmoc-[S]-3-amino-3-(2-nitrophenyl)-propionic acid (first coupling 200 μl; second coupling 100 μl) were distributed to the reaction vessels. After 1 h coupling time, coupling reagents were filtered off and the resin was washed with DMF (1×200 μl) followed by a second coupling step (1 h). Amino acids were introduced using a sevenfold molar excess of the respective Fmoc-L-amino acid. After washing with DMF (4×400 μl) Fmoc deprotection was carried out two times, 10 min each, with 30% piperidine in DMF (300 μl). Nine washing steps were done with DMF (300 μl).

Coupling of the carboxy-tris-NTA(O*t*Bu) to the free *N*-termini was done manually at room temperature in the dark. The resins were incubated twice with 3 eq. carboxy-tris-NTA(O*t*Bu), 3 eq. O-(1H-benzotriazole-1-yl)-N,N,N′,N′-tetramethyluronium tetrafluoroborate (TBTU), 3 eq. HOBt, and 5 eq. N,N′-Diisopropylethylamine (DIPEA) in DMF for 16 h. For a third coupling step, the amounts were reduced to 1 and 2 eq. (referred to the free peptide amino groups before coupling), and the reaction time to 8 h. The intermediate washing steps were performed with DMF, and the completeness of the coupling was analyzed by a KAISER test (2). Cleavage of the peptides from the resins as well as side chain deprotection were done in a single step using a mixture of 1.25% water, 1.25% triisopropylsilane and 1.25% ethanedithiol in trifluoracetic acid (TFA). The resins were incubated for 4 h at room temperature in the dark, filtered and washed with TFA. Soluble compounds were removed in vacuum followed by precipitation of the cleaved peptides with cold diethylether. The precipitated peptides were pelleted by centrifugation and washed three times with cold diethylether. Purification of the crude peptides was via reversed-phase HPLC using a C_{18}column (Vydacfi 218TP, Grace) and a linear gradient of 0–30% acetonitrile in water containing 0.2% TFA. The purified peptides were lyophilized, analyzed by ESI-MS, and stored at −80 °C until use. Indicated are the masses from the deconvoluted mass spectra.

Photocleavage. The AC(S*t*Bu)SGGG*Anp*SGGGHHHHH was dissolved in HBSE-buffer (20 mM Hepes, 150 mM NaCl, pH 7.5, 50 μM EDTA) to a final concentration of 2 mg/ml. For each time point, 120 μL of the solution was illuminated in a 24-well plate on ice using 366 nm light (2×8 W, Benda). The cleavage reaction was monitored by reversed-phase HPLC using a C_{18} column (Vydac 218TP, Grace). Elution was performed using a linear gradient of 0–29% acetonitrile in water containing 0.2% TFA. Absorption was monitored at 220 and 270 nm.

PA tris-NTA labeling and nickel loading. For fluorescence labeling, the peptides (1 mM) were incubated with 1.2 eq. ATTO565-maleimide in 20 mM Hepes, pH 7.0 for 2 h at room temperature in the dark. Purification was via reversed-phase HPLC using a C_{18} column (Vydac 218TP, Grace) and a linear gradient from 0–35% acetonitrile in water containing 0.2% TFA. Fluorescently labeled PA tris-NTAs were identified by ESI^- mass spectrometry. Lyophilized compounds were incubated with a 15-fold molar excess of Ni^{2+} ions for 30 min at pH 7.0. The excess of Ni^{2+} was removed by anion exchange chromatography (HiTrap Q, GE Healthcare) at pH 7.0 (loading buffer: 10 mM Hepes, pH 7.0; elution buffer: 10 mM Hepes, 1 M NaCl, pH 7.0). The PA tris-NTA concentration was determined via the absorption of the ATTO565 dye ($A_{max} = 563$ nm, $\lambda_{max} = 120,000\ L\,mol^{-1}\,cm^{-1}$).

Protein purification. His_6- and His_{10}-tagged maltose-binding proteins (MBP) were expressed, purified, and labeled as described (3, 4). Fluorescence labeling was performed using N-hydroxysuccinimidyl (NHS) dyes. Alternatively, single cysteine MBP mutants were labeled by maleimido fluorophors.

Very-low density lipoprotein receptor (VLDLR) derivative and human rhinovirus serotype 2 (HRV2). Expression and purification of the pentameric concatemer of ligand-binding module 3 of human VLDLR and the isolation of HRV2 particles were as described elsewhere (5, 6). Fluorescence labeling of HRV2 was achieved by chemically modifying surface-exposed lysines with the amino-reactive dye Cy5. The crystal structure of the virus (7) indicates that this can involve up to 240 residues per virion; most of them belong to the extensively exposed capsid protein VP1. Preferential labeling of VP1 was indeed confirmed by SDS-PAGE (8). A key player in receptor binding is lysine 224 of VP1 (9). Under the chosen labeling conditions, receptor binding and biological activity of the virus (i.e. infectivity) were only slightly reduced (8, 10). The receptor used in these experiments was a pentamer of repeat 3 of VLDLR (5), with the modules concatenated in a head to tail fashion (11). To ease expression and purification, this recombinant receptor was fused to MBP at the *C*-terminus and carried a His_6-tag at the *N*-terminus (MBP-V33333-H_6). HRV2 was labeled with Cy5 *N*-hydroxysuccinimidyl esters following the described protocol (12). The original aim was to mimic the natural receptor (composed of eight similar but not identical modules) and at the same time to remove bias in the

interpretation of affinity measurements possibly originating from differences in the binding strength of the different receptor modules. The multivalent nature of the interaction between virus and receptor implicates that loss of interaction between symmetry-related binding sites on the virion and some of the five receptor modules only results in a decrease in avidity but is not expected to abolish binding (11, 13).

Surface preparation for fluorescence microscopy. In each preparation step, two glass cover slips (24 mm diameter, thickness 160–190 μm, Menzel) were paired face-to-face. After each chemical modification, the chips were rinsed thoroughly with appropriate solvents and dried in a nitrogen stream. First, the cover slips were cleaned for at least 1 h in Piranha solution [H_2SO_4 : H_2O_2 (30%), 2:1]. Directly afterwards, they were silanized with (3-glycidyloxypropyl) trimethoxysilane for 1 h at 75 °C. In the next step, diamino-PEG (2000 Da) was coupled to the surface overnight at 75 °C. The maleimide function was introduced by incubation of the surfaces with a concentrated solution of 3-(maleimido)propionic acid *N*-hydroxysuccinimide ester in DMF for 1 h at room temperature. Finally, the tris-C*Anp*H_5 was coupled via the cysteine by incubation with 1 mM peptide in HBS buffer for 1.5 h. Unreacted maleimide functionalities on the surface were deactivated with 50 mM cysteine in HBS. The dried chips were stored at −20 °C for up to two weeks.

1. Lata S, Reichel A, Brock R, Tampé R, and Piehler J (2005) High-affinity adaptors for switchable recognition of histidine-tagged proteins. *J Am Chem Soc* 127:10205–10215.
2. Kaiser E, Colescott RL, Bossinger CD, and Cook PJ (1970) Color test for detection of free terminal amino groups in the solid-phase synthesis of peptides. *Anal Biochem* 34:595–598.
3. Lata S and Piehler J (2005) Stable and functional immobilization of histidine-tagged proteins via multivalent chelator headgroups on a molecular poly(ethylene glycol) brush. *J Anal Chem* 77:1096–1105.
4. Reichel A, *et al.* (2007) Noncovalent, site-specific biotinylation of histidine-tagged proteins. *Anal Chem* 79:8590–8600.
5. Ronacher B, Marlovits TC, Moser R, and Blaas D (2000) Expression and folding of human very-low-density lipoprotein receptor fragments: Neutralization capacity toward human rhinovirus HRV2. *Virology* 278:541–550.
6. Hewat EA, *et al.* (2000) The cellular receptor to human rhinovirus 2 binds around the 5-fold axis and not in the canyon: A structural view. *EMBO J* 19:6317–6325.
7. Verdaguer N, Blaas D, and Fita I (2000) Structure of human rhinovirus serotype 2 (HRV2). *J Mol Biol* 300:1179–1194.
8. Kremser L, Okun VM, Nicodemou A, Blaas D, and Kenndler E (2004) Binding of fluorescent dye to genomic RNA inside intact human rhinovirus after viral capsid penetration investigated by capillary electrophoresis. *Anal Chem* 76:882–887.
9. Verdaguer N, Fita I, Reithmayer M, Moser R, and Blaas D (2004) X-ray structure of a minor group human rhinovirus bound to a fragment of its cellular receptor protein. *Nat Struct Mol Biol* 11:429–434.
10. Kolivoska V, *et al.* (2007) Electrophoresis on a microfluidic chip for analysis of fluorescence-labeled human rhinovirus. *Electrophoresis* 28:4734–4740.
11. Moser R, *et al.* (2005) Neutralization of a common cold virus by concatemers of the third ligand binding module of the VLDL-receptor strongly depends on the number of modules. *Virology* 338:259–269.
12. Kremser L, Konecsni T, Blaas D, and Kenndler E (2004) Fluorescence labeling of human rhinovirus capsid and analysis by capillary electrophoresis. *Anal Chem* 76:4175–4181.
13. Wruss J, *et al.* (2007) Attachment of VLDL receptors to an icosahedral virus along the 5-fold symmetry axis: Multiple binding modes evidenced by fluorescence correlation spectroscopy. *Biochemistry* 46:6331–6339.

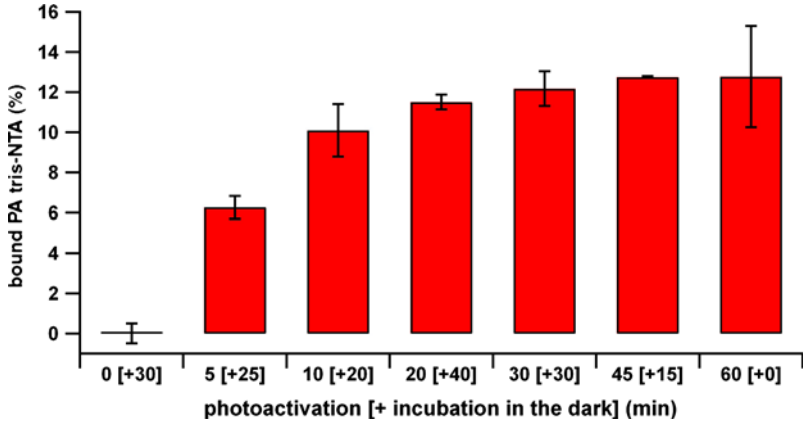

Fig. S1. Percentage of MBP-H_6 bound to PA tris-NTA-His_5 as function of the illumination and subsequent incubation time. MBP-H_6 and ATTO565-labeled PA tris-NTA-His_5 were incubated in a 1:1 molar ratio. The complex formation was analyzed by size exclusion chromatography as described in the main text. Data are derived from triplicate measurements; error bars represent standard deviations of the mean.

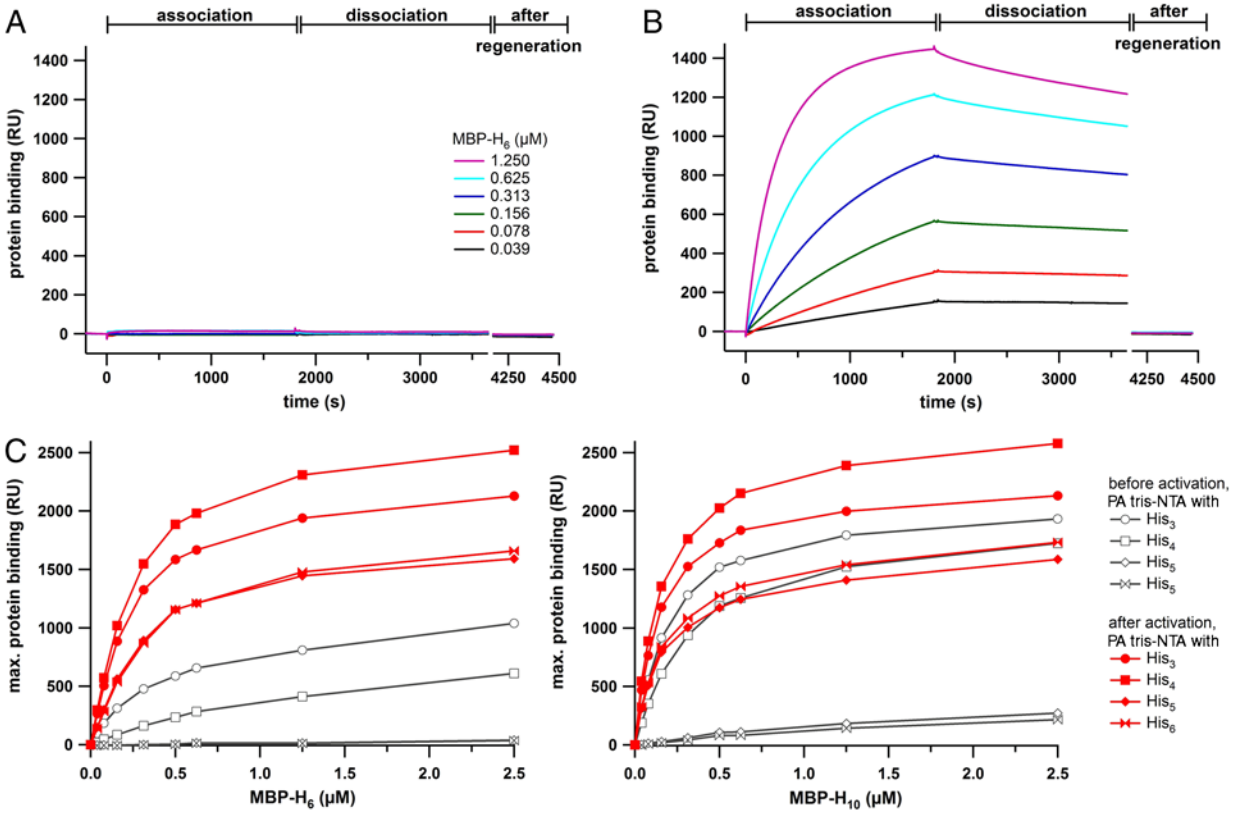

Fig. S2. The association and dissociation kinetics of MBP-H_6 before (*A*) and after photoactivation (*B*) reveal similar to the MBP-H_{10} experiments (compare Fig. 3 *A* and *B*) a dramatic shift in affinity. However, the overall affinity of MBP-H_6 is in comparison to MBP-H_{10} somewhat lower since the His-tag onto the MBP-H_6 protein is four histidines shorter. The changes in affinity have a predominant effect on the observed off-rate after photoactivation. (*C*) Maximum protein binding signals before (open symbols) and after (closed symbols) photoactivation of the different PA tris-NTAs are plotted against MBP-H_6 (left) and MBP-H_{10} concentrations (right). Variations in the maximum protein binding after photoactivation are due to different amounts of immobilized PA tris-NTA.

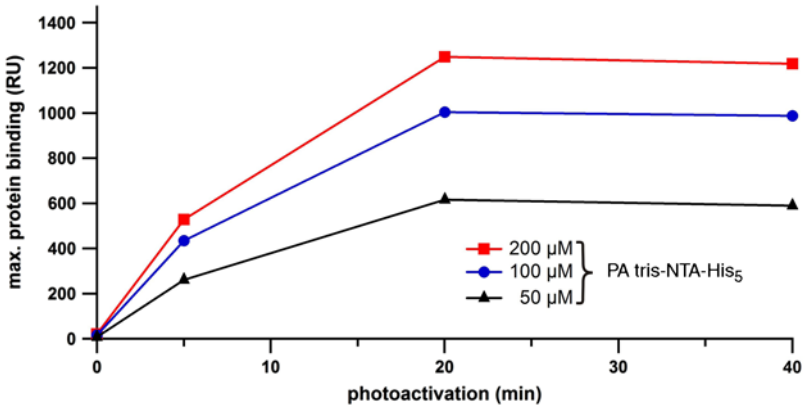

Fig. S3. Maximum protein binding for MBP-H_6 investigated by surface plasmon resonance measurements. CM5 sensor chips were functionalized with different concentrations of PA tris-NTA-His_5 (50–200 μM). Binding of MBP-H_6 (1.25 μM) was monitored before (0 min) and after different progressive illumination times (5, 20, 40 min).

Table S1. Molecular masses of the PA tris-NTAs

Peptide	Molecular formula	Mass (calculated)	*m/z*
PA tris-NTA-His_3	$C_{92}H_{128}N_{28}O_{42}S$	2,330.23	2,331.05[M + H^+], 2,393.00 [100%], 2,455.06, 2516.92
PA tris-NTA-His_4	$C_{98}H_{135}N_{31}O_{43}S$	2,467.37	2,468.00[M + H^+, 100%], 2,531.57, 2,592.86
PA tris-NTA-His_5	$C_{104}H_{142}N_{34}O_{44}S$	2,604.51	2,605.16[M + H^+, 100%], 2,668.08, 2,703.13, 2,731.86
PA tris-NTA-His_6	$C_{110}H_{149}N_{37}O_{45}S$	2,741.65	2,742.67[M + H^+, 100%], 2,764.67, 2,786.14, 2,807.43, 2,829.36